Front Page

Project no. LSHB-CT-2004-005137
Project acronym: BioSim
Project title: Biosimulation – A New Tool in Drug Development

Instrument: Network of Excellence
Thematic Priority: Genomics and biotechnology for health

D62. Refined computer model for representative model substrates with yeast.

Due date of deliverable: Month 15
Actual submission date: 26.08.2005

Period covered: from December 1, 2004 to 30 November 2005

Start date of project: 1 December 2004 End of project: 30 November 2009

Partner name: Martin Bertau
Organization name of lead contractor for this deliverable: Technical University of Dresden

Project co-funded by the European Commission within the Sixth Framework Programme (2002-2006)

Dissemination Level : PU Public

Deliverable D62

Refined computer model for representative model substrates with yeast.

L. Brusch[1], J. Smolinski[1] , K. Leppchen[1], M. Katzberg[1],G. Jörg[1], M. Bertau[1], F. Mensonides[2] , and U. Kummer[2]

[1] Dresden University of Technology, Institute of Biochemistry, 01062 Dresden, Germany, Partner #19

[2] EML Research gGmbH, Bioinformatics and Computational Biochemistry, EML, 69118 Heidelberg, Germany, Partner #27

Summary. Chemo- and stereoselectivity of drug metabolism are greatly affected by xenobiotic cell-stress exerted by the active pharmaceutical ingredient. Stress-induced competing cellular processes like *retro*-Claisen condensation, ester hydrolysis and dehalogenation generate metabolites which interfere with different enzyme activities, above all the glycolytic network, and cause the cell to alkylate the substrate. The competing processes have been implemented into the model.

1. Introduction

In drug development potential metabolic fates of pharmaceutically active compounds (PAC) inside living cells play an important role. It is not the stereo-geometry of PACs alone which is affected by cellular metabolism, but also chemical integrity of a PAC is greatly influenced by cellular metabolic activity as well as stress physiology.

As model PACs three ketones are considered: ethyl acetoacetate (**AEE**), ethyl 4-chloro-acetoacetate (**4CAEE**) and ethyl 4,4,4-trifluoro-acetoacetate (**FAEE**) the chemical structures of which are given in Figure 1.

Hoever, there exists no knowledge of how these compounds are being metabolised by living cells. In Deliverable 61 we have introduced a preliminary model for **AEE** which was able to predict the stereoisomer distribution in **HBE** in dependence of ketone concentration and the amount of sugar added.

In this Deliverable, a refined is capable of dealing also **FAEE** and **4CAEE**. In addition the metabolic pathways of xenobiotic biotransformations were elucidated and implemented into the refined model.

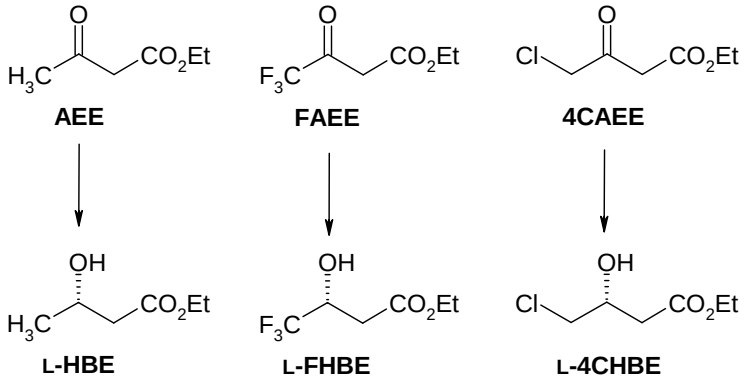

Figure 1. Model PAC studied.

2. Approach

The modelling approach pursued in this workpackage implies two critical layers of abstraction. First of all, a PAC which is mostly administered perorally will face the gastro-intestinal microbial barrier by which the drug compound is actively metabolised prior to resorption by the gut mucosa. The fraction of the active pharmaceutical ingredient (API) which is metabolised during the gastro-intestinal passage is mostly unknown. Likewise there is no knowledge of the metabolites formed in the course of this process. Yet, these gastro-intestinally produced metabolites enter the hepatic blood stream where they then are subject to the biotransformatory activity of the liver. Of these reactions phase I / phase II metabolism is the best studied system. However current approaches lack information on micro-metabolites which themselves may be highly physiologically active, but are undetectable in the high dilution in a mammalian body.

For these reasons the metabolism of three model compounds was studied with the model organism *Saccharomyces cerevisiae*. Since the biotransformation of a drug compound occurs in the cytosol, and as the most important cytosolic metabolic pathway affected by the presence of a xenobiotic compound in the cell, we have introduced biological abstraction. All cell types the API is facing until its excretion are generally regarded as cytosols in which glycolysis is affected. Thus, xenobiotic metabolism is not dependent on the cell type on this level of abstraction. Therefore *S. cerevisiae* can be used to reflect the metabolism of the model compounds irrespective of whether enzymic degradation occurs in the intestine (anaerobic) or in the liver.

3. Experimental Section

3.1. General

Baker's yeast (*Saccharomyces cerevisiae* L13) was the product of Societé industrielle de levure FALA, Strasbourg, France, and was obtained from the local

subsidiary in Kesselsdorf, Germany. Chemicals and organic solvents were obtained from Fluka (Buchs, CH) and Acros (Geelen, Belgium). Sucrose was obtained from a local store.

Product identity was confirmed by NMR spectroscopy. ^{1}H-NMR spectra were recorded in $CDCl_3$ with a Bruker DRX-500 spectrometer at 500 MHz. Chemical shifts are quoted in ppm from internal TMS or TSP. Absolute configuration was determined using a Carl Zeiss Jena polarimeter Polamat A (c=1.0, $CHCl_3$) and by comparison of the obtained results with published data. All reactions were monitored by GC using an Analytik Jena Perichrom GC ST200. Conversions, yields and stereoisomer distributions were determined by GC, metabolite identification was done by GC/MS.

3.2. Determination of the extent of conversion

The conversions were measured using a J&W Scientific DB-5 column (30 m, 0.25 mm I.D.). The pressure of N_2 gas was 80 kPa; the temperatures of the injector and the detector were 240°C and 250°C, respectively. The % conversions were determined using an integrator.

3.3. Determination of optical purity

For the determination of enantiomeric excess (ee) and diastereomeric excess (de) the pure β-hydroxy esters were converted into the corresponding trifluoro acetates by reacting with a 1.2 molar amount of trifluoro acetic acid anhydride in dry CH_2Cl_2 at 65°C. After the reaction was complete, the volatile components were evaporated. GC analysis of the resulting trifluoro acetate was conducted using a chiral column as indicated below. The trifluoro acetoacetates of $NaBH_4$ reduced material were used to find the suitable conditions for chiral GC analysis. The pressure of N_2 gas was 130 kPa; the temperatures of the injector and the detector were 240°C and 250°C, respectively. The relative amounts were determined using an integrator.

3.4. Determination of the cell vitality

Cell vitality was examined by the methylene blue method (Crotti et al., 2001). At each time point indicated an aliquot of cells was taken from the reaction mixture and stained with 0.01% methylene blue. The number of stained and unstained cells was determined by microscopy. A minimum of 200 cells was counted for each measure.

3.5. Whole-cell biotransformation

To a fermenter containing tap water (10 l) were added Fala baker's yeast (200 g) and sucrose (200 g). After incubating for 20 min. at 30.0°C, to the aerated culture (2.0 l/l·min) substrate as indicated below was fed continuously for 20 h, while pH was kept at 6.3. The reaction was monitored by GLC analyses. After 20 h the biomass was removed by centrifugation at 4.0°C, the yeast was washed with water, and the combined aqueous phase was incubated for 18 h with 7500 U *Bacillus subtilis* protease (pronase E)

according to the method by Jörg et al. (2004). After extraction with diethyl ether (3 x 1.0 L), the organic extracts were dried over $MgSO_4$, filtered, and concentrated *in vacuo*.

3.5.1. AEE

Substrate:

AEE (450 ml, 462.6 g, 3.556 mol).

Conversion:

Ramp from 130°C to 150°C with 2°C/min. The keto-substrate **AEE** and products **L-HBE** and **D-HBE** were observed at retention times of 5.5 min and 7.1 min, respectively.

Enantiomeric excess:

Macherey & Nagel Lipodex E column (50 m, 0.25 mm I.D.) isothermal 95°C. The (*R*)-carbinol **D-HBE** was observed at a retention time of 6.6 min and the (*S*)-enantiomer **L-HBE** at 7.3 min.

Yield:

Pure **L-HBE** (314,8 g, 2.382mol, 67%) with an ee of 98% (*S*) was obtained as a colourless liquid.

3.5.2. 4CAEE

Substrate:

4CAEE (250 ml, 302.0 g, 1.835 mol).

Conversion:

Ramp from 75°C to 130°C with 5°C/min. The keto-substrate **4CAEE** and products **L-4CHBE** and **D-4CHBE** were observed at retention times of 3.5 min and 6.1 min, respectively.

Enantiomeric excess:

Macherey & Nagel Lipodex A column (50 m, 0.25 mm I.D.) using a rate of 10°C/min. from 80°C up to 180°C, then with the column at 180°C for 3 min. The (*S*)-carbinol **D-4CHBE** was observed at a retention time of 8.8 min and the (*R*)-enantiomer **L-4CHBE** at 9.6 min.

Yield:

Pure **L-4CHBE** (183.1 g, 1.098 mol, 60%) with an ee of 54% (*R*) was obtained as a colourless liquid by column chromatography (CH_2Cl_2:ethyl acetate = 9:1).

3.5.3. FAEE

Substrate:

FAEE (100 ml, 126.0g, 684 mmol).

Conversion:

50°C (isothermal). The keto-substrate **FAEE** and products **L-FHBE** and **D-FHBE** were observed at retention times of 3.7 min and 5.5 min, respectively.

Enantiomeric excess:

Macherey & Nagel Lipodex A column (50 m, 0.25 mm I.D.) running a ramp from 60°C to 120°C with 10°C/min. The (*S*)-carbinol **D-FHBE** was observed at a retention time of 9.1 min and the (*R*)-enantiomer **L-FHBE** at 10.2 min.

Yield:

Pure **L-FHBE** (46.4 g, 250 mmol, 36.5%) with an ee of 62% (*R*) was obtained as a colourless liquid.

4. Results and discussion

4.1. Whole-cell Biotransformation

When ketones **AEE**, **FAEE** and **4CAEE** were submitted to stereoselective reduction by respiro-fermenting *S. cerevisiae*, the respective carbinols were obtained. In addition from **4CAEE** also the dehalogenation product **L-HBE** was found, and all ketones reacted to give the *retro*-Claisen products and the respective acetones as a result of decarboxylation which occurred consecutively to ester hydrolysis..

Figure 2 gives a schematic overview of these competing pathways with the example of **4CAEE**: (i) Nucleophilic substitution of the chloro substituent at C-2 by GSH initiates dehalogenation (Jörg & Bertau, 2004). Three dissimilar pathways result from semi-thioacetal formation: (ii) liberation of chloride by nucleophilic thiolysis of the thioether bond and production of ethyl acetoacetate (**AEE**), (iii) cleavage of the carbon backbone (*retro*-Claisen condensation) to give chloroacetate and ethyl acetate, or (iv) dissociative loss of GSH or hydrolysis to give ketone and enol, respectively. (v) Nucleophilic attack of GSH at the ester carbon leads to ester hydrolysis which is followed by decarboxylation to give chloro acetone .

Recent studies had revealed that dechlorination of **4CAEE** is a novel type of glutathione-dependent dehalogenation which is catalysed by a so far unidentified glutathione-dependent dehalogenase (Jörg & Bertau, 2004) (Figure 3). Our investigations aimed to elucidate the mechanisms of further side-reactions encountered in the course of the microbial reduction of **4CAEE** and their causes: (i) *retro*-Claisen condensation and (ii) ester hydrolysis.

Due to its high alkylating power, **4CAEE** is reactive towards GSH, i.e. it exerts xenobiotic stress (Penninckx, 2000, De Kimpe et al., 1987). As the dechlorination is mediated by cytosolic glutathione (GSH), we studied the participation of GSH and/or a glutathione *S*-transferase (GST) in the other side reactions.

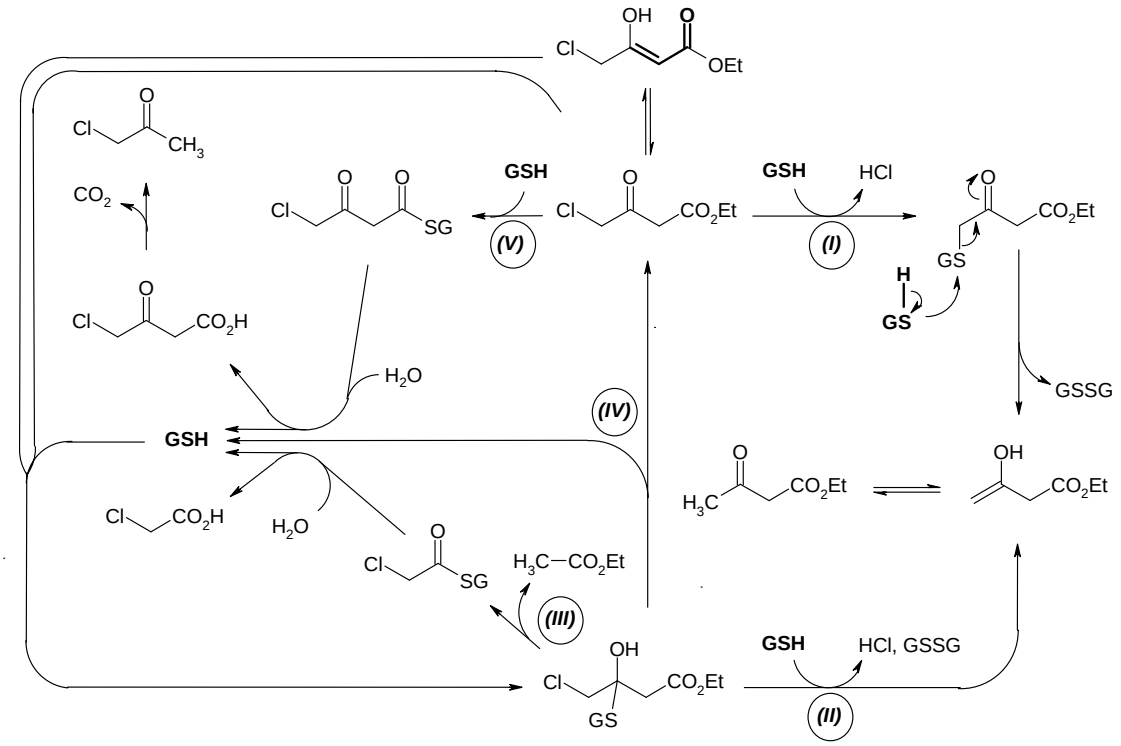

Figure 2. The example 4CAEE shows that besides stereoselective reduction there exist competing pathways in *S. cerevisiae* as a result of xenobiotic cell stress: (i) Dehalogenation after attack of GSH at C-4, (ii) dehalogenation, (iii) *retro*-Claisen condensation, (iv) de-glutathionylation, and (v) ester hydrolysis. The susceptibility of the Michael system for nucleophilic 1,4-addition renders also the enol a substrate for dehalogenation. A full scheme in given in the annex.

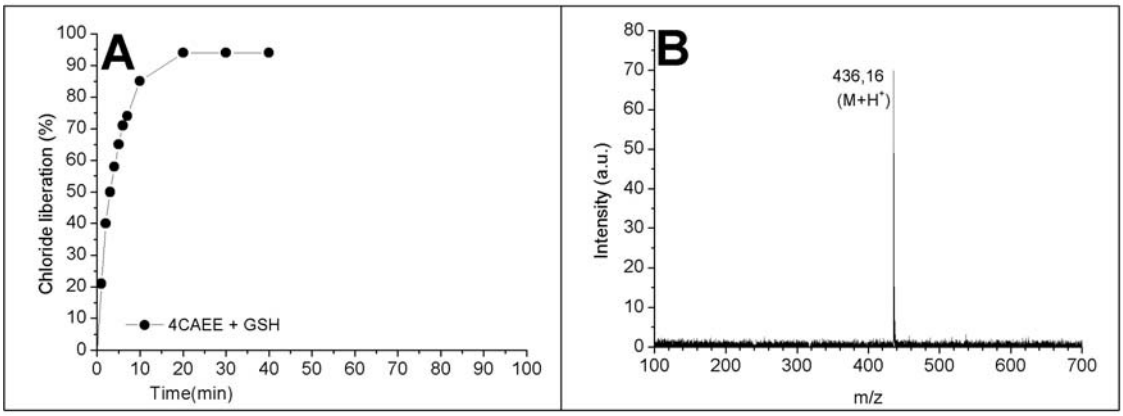

Figure 4. Nucleophilic attack of glutathione (GSH) at the the terminal C in 4CAEE is responsible for substrate dehalogenation. The liberation of chloride has been proven by determination of inorganic chloride (A). The LC/MS spectrum of ethyl 4-glutathionyl acetoacetate proves the involvement of stress metabolit GSH in xenobiotic metabolism of chlorinated substrates (B).

4.2. *Retro*-Claisen condensation

In our experiments up to 14% of the starting material reacted by hydrolytic cleavage of the carbon backbone. According to a report by Grogan et al. (2001), this reaction-type may be mediated by hydrolases, e.g. by 6-keto-campher hydrolase. However, there were no indications that this side-reaction proceeds enzymatically. Therefore, with respect to the alkylating properties of the substrate, we investigated the contribution of the cell-stress protectant glutathione (GSH) to this process.

As outlined in figure 2, formation of *retro*-Calisen-products proceeds via glutathione addition to the carbonyl centre. However, this intermediate could not be identified directly by LC/MS methods, what is ascribed to the relative lability of the semi-mercaptal with a life-time too short for detection under LC/MS conditions.

Clear evidence for the emergence of these species was provided by the LC/MS-analytical identification of bis-thioacetal which was formed in trace-amounts (≤ 1%) from the keto esters *via* the unstable semi-thioacetal (Figure 4).

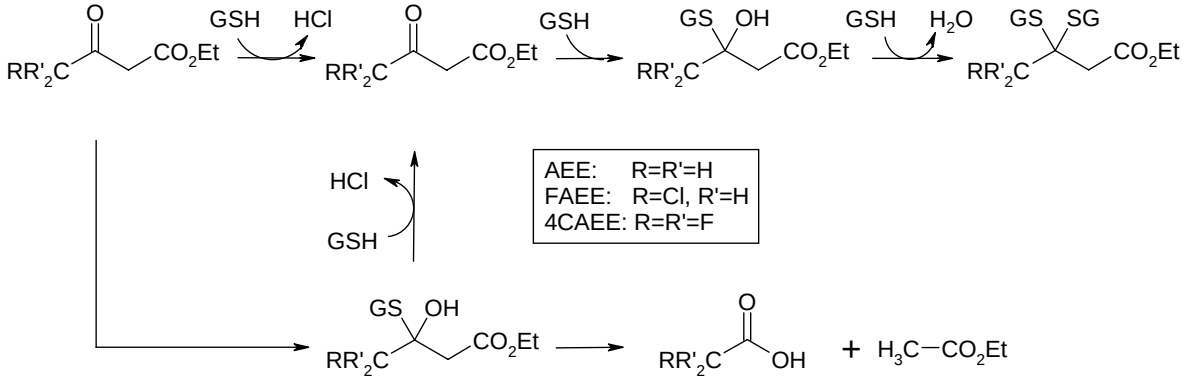

Figure 4. Reactions of GSH with the β-keto group. Bis-glutathionylation was observed only for non-halogenated species, since dehalogenation of semi-thioacetal is the faster process.

Formation of bis-glutathionyl thioacetal appears plausible, since conversion of carbonyls in thioacetals is a common method in protective group chemistry (Naik et al., 2004; Sartori et al., 2004). Attempts to directly demonstrate bis-glutathionylation of **4CAEE** failed, because dehalogenation and *retro*-Claisen condensation were the faster processes. Here bis-glutathionylation of the β-keto group will not take place, until the α-chlorine substituent has been removed. Since for the other species bis-glutathionylation and *retro*-Claisen condensation were observed, these results also demonstrated that halogen substitution is not a prerequisite for these cell-stress associated by-processes to occur.

Another proof for semi-thioacetal formation was provided by the emergence of ethyl semiacetals and enol ethers which were detected upon GC/MS analysis of the reaction mixture. In experiments with whole-cells as well as with cell liquor, glucose catabolite ethanol was sequestering the intermediate carbenium ion which had been

formed in the course of the backward reaction to give semi-acetal **19** in trace amounts (≤ 1%). Thermal loss of water under GC/MS conditions afforded the enol ether (Figure 5).

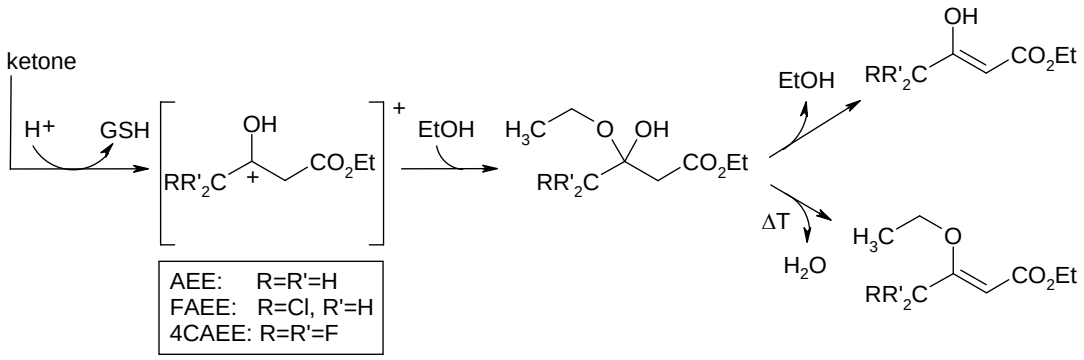

Figure 5. De-glutathionylation of semi-mercaptals promotes enolisation as well as formation of semi-acetals by sequestration of the intermediary carbenium ions with fermentatively produced ethanol. These pathways are purely microbial since hepatic metabolism produces lactate under oxygen limitation.

The structures of the enol ethers were confirmed by comparison of GC/MS data with chemically synthesised material. This experiment also demonstrated the involvement of a nucleophilic agent like GSH in their formation. Aqueous mixtures of ketone and ethanol alone remained unaltered, whereas the reaction set in immediately, when GSH or *N*-acetyl cysteine (NAC) was added. Once the ethyl semiacetals has been formed, there are three pathways to further react: (i) cleavage of the carbon backbone (*retro*-Claisen condensation), (ii) dissociative loss of GSH or hydrolysis respectively, or (iii) with chlorinated compounds liberation of chloride by nucleophilic thiolysis of the thioether bond and production of dehalogenation product ethyl acetoacetate (**AEE**) (Figure 2,3).

GST catalysis as well as yeast cell liquor were not found to significantly increase the *retro*-Claisen reaction rate.

The active role of GSH in cell-stress mediated *retro*-Claisen condensation was demonstrated with GSH-depleted cells. After treatment with *N*-ethyl maleimide (NEM) according to the method by Datta & Samanta (1992) no *retro*-Claisen product was detectable. The same applied for NEM-treated cell-liquor.

4.3. Ester hydrolysis

Saponification of the ester group is a common yield-limiting complication in whole-cell biotransformations and has hitherto been assigned to the action of hydrolases (Chin-Joe et al., 2000; Breeuwer et al. 1995). This process yields ethanol and the respective acetone; the unstable intermediary β-keto acid was not observed. Ethanol was not quantified, as it is also a regular metabolite of the yeast cell. We found that the occurrence of ester hydrolysis is another example for the implications of GSH on the

metabolic fate of β-keto esters. GSH catalysed saponification of the substrate is a sequence of thiolysis and subsequent hydrolysis of the unstable thioester (Figure 2.).

Both saponification of keto substrate and decarboxylation of β-keto acid need not necessarily be enzyme catalysed: The latter was shown to be a spontaneous process, and ester hydrolysis can proceed also abiotically by the action of the nucleophile GSH alone (Jörg et al., 2005). In experiments in cell-free culture-medium no ester hydrolysis occurred, while whole cells which were depleted from GSH by addition of *N*-ethyl maleimide (NEM) (Datta & Samanta, 1992) did hydrolyse the substrate as the result of background esterase activity.

The interplay between GSH mediated hydrolysis and hydrolase activity was nicely demonstrated with the hydrolytic release of fluorescein from fluorescein diacetate (Schnürer & Rosswall, 1982; Guilbault & Kramer, 1964). The fluorescence properties of the saponification product allowed quantifying the contributions of GSH and intracellular hydrolases in whole-cell hydrolyses of xenobiotics (Figure 6).

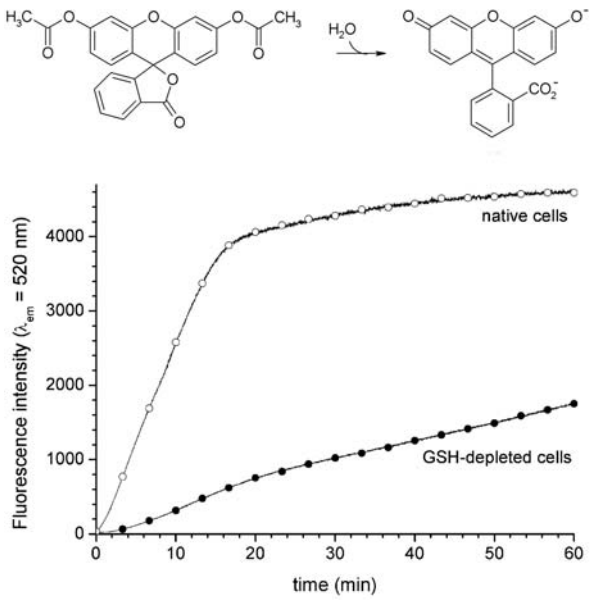

Figure 6. Intracellular hydrolytic activity of yeast cells in whole-cell biotransformations is primarily the consequence of elevated cytosolic GSH levels due to xenobiotic cell stress (68%). Experiments with GSH-depleted cells revealed that only 32% of the overall hydrolytic activity could be ascribed to hydrolase activity.

As was shown by measuring the overall hydrolytic activity in native and GSH-depleted cells, substrate hydrolysis was primarily the product of the action of GSH on the xenobiotic substrate (68%). Only 32% of the hydrolytic activity was attributable to hydrolases.

In untreated cells cytosolic GSH levels varied between 1 and 9 mmol/l, what is in accordance with values (1-11 mmol/l) reported by Schäfer & Büttner (2001). Under cell-stress conditions, where cytosolic GSH was measured to amount up to 30 mmol/l, the

action of a glutathione *S*-transferase was not necessarily required for GSH-mediated substrate hydrolysis to occur. Hydrolysis of fluorescein was almost complete after 20 min. *In vitro* experiments with 30 mM GSH proceeded likewise. With lower intracellular GSH levels however, GST-activity became increasingly effective. Where GSH concentration was 1 mM or lower, hydrolytic release of fluorescein Diacetate was negligible, unless there was catalytic support by a GST. In whole cells ester hydrolysis experienced a rate enhancement of 59% under GST catalysis. The same applied for yeast cell liquor.

Hence, the overall hydrolytic activity of a xenobiotically stressed cell is the sum of abiotic GSH-mediated hydrolysis, GST-catalysed hydrolysis and the action of intracellular hydrolases.

4.4. Competing pathways and stereoselectivity

Ethyl 4-chloro-acetoacetate (**4CAEE**) and chloro-acetone are alkylating agents (De Kimpe et al., 1987). This property is of special importance, when the substrate is being reduced stereoselectively by reductases with an essential reactive sulfhydryl function. The sulfhydryl groups are inhibited irreversibly by alkylation through the α-halogen carbonyl compound (Ushio et al., 1991). As in living cells different enzymes with different stereoselectivities compete for the substrate, selective inhibition of sulfhydryl enzymes by these reagents considerably affects stereoisomer distribution in the product.

This was nicely outlined with the observed unusual high enantiopurity of dehalogenation consecutive product ethyl (S)-3-hydroxybutyrate (**L-HBE**). Saponification product chloro acetone is an inhibitor of D-directing β-ketoacyl reductase of the fatty acid synthase (FAS) complex (EC 1.1.1.100) (Ushio et al., 1991, Wakil et al., 1983). We found that as a consequence of enzyme inhibition dehalogenation product **AEE** was reduced to β-hydroxy ester **L-HBE** with >99.5% ee. For comparison, in our experiments where **AEE** was submitted directly to microbial reduction with *S. cerevisiae*, **L-HBE** was obtained with 98% ee.

By depletion of the cytosolic GSH-pool, fission product chloroacetic acid which is formed from **4CAEE**, acts as an inhibitor of the glutathione-dependent processes. But the *retro*-Claisen product also has a bearing on product stereopurity, since the alkylating agent also affects stereoselectivity of the biotransformation by binding to essential sulfhydryl groups in the active sites of dehydrogenases (Nakamura et al., 1990). Chloroacetic acid was detected in up to 10 mmol/l; stereodirecting effects became effective already at concentrations ≥ 3 mmol/l.

Table 1. GSH promotes formation of enol from β-keto ester AEE.

Entry	GSH	Enol-form	Keto-form
1	+	30%	70%
2	-	17%	83%

Due to the reactivity of the β-carbonyl group towards thiols, under cell stress conditions (c_{GSH} = 30 mmol/l) GSH promoted formation of enols from β-keto esters. Since especially electron deficient species are subject to GSH-mediated reactions, this effect was measurable only for the non-halogenated species **AEE**. In potassium phosphate buffer, at pH 6.5, the equilibrium fraction of the enol form was determined as 17%. Under cell stress conditions an increase to 30% within 8 min. was observed (Table 1).

4.5. Inhibition of competing reaction pathways

All side reactions described in this contribution were mediated by the action of cell-stress protectant glutathione, and they have in common their irreversibility, for bond breakage prevents back reaction. When the cells were thoroughly depleted from GSH by adding *N*-ethyl maleimide (NEM) (Datta & Samanta, 1992) no by-product formation was observed, what clearly proves the involvement of GSH in these competing pathways.

5. Modelling

In order to obtain an overall view of these stress response pathways, we decided to analyse the stoichiometric matrices of three comprehencive reaction networks (see appendix) by means of elementary flux mode analysis (Schuster et al. 1999). The pathway of 4CAEE-catabolism includes 117 reactions many of which are reversible. Using the modeling platform Copasi we encoded the reaction network in the language SBML and calculated the elementary flux modes, i.e. minimum sets of reactions that can operate simultaneously at steady state. We discovered 4 such modes for degradation of 4CAEE without the net consumption or production of redox equivalents. These 4 modes produce the final metabolites ethyl 3-ethoxy-4-chloro-2-butenoate, ethyl 3,3-bisethoxy-4-chlorobutanoate, oxol-2,4-dione, 2,4-bischloromethyl-3,5-bisethoxycarbonyl-4-methyl pyridine.

It is remarkable that such modes do not depend on or disturb the glycolytic activity of the cell. The latter is depending on and contributing to the regulation of the cellular redox balance. Our analysis also revealed 20 other elementary modes of 4CAEE degradation that do consume NADH and therewith interfere with glycolysis (Deliverable D61). In order to facilitate these additional modes over a longer duration, the cell has to ensure the necessary reproduction of NADH which under anaerobic conditions may proceed via the secretion of acetaldehyde or succinate. Our analysis has shown that the production of cytotoxic intermediates along this large set of stress response modes appears likely on the basis of the stoichiometric data.

We obtained similar qualitative results for the cellular stress responses to AEE and FAEE. This large scale analysis is complementing the detailed quantitative analysis of the metabolic oscillations in the glycolysis core model perturbed by the main reactions in response to the xenobiotic.

6. Conclusion

Numerous effects have been shown to act on simple xenobiotics. The metabolites arising from these reactions are in physiologically active. For instance chloro acetone which acts as an enzyme inhibitor may greatly interfere with hepatic isomerisation processes as they take place e.g. with ibuprofene. In other words, we have shown that it is indispensable to investigate pharmaceuticals for micro-metabolite production already in the intestine, since otherwise deleterious consequences for the patient may occur.

After the spectra of metabolic pathways had been elucidated for the three model compounds **AEE**, **FAEE** and **4CAEE**, these data were implemented into the mathematical model. This refined model now allows more detailed predictions of the stereoisomer distribution in the products.

7. References

Bertau, M., Bürli, M., Hungerbühler, E. and Wagner, P. (2001) A novel highly stereoselective synthesis of chiral 5- and 4,5-substituted 2-oxazolidinones. *Tetrahedron: Asymmetry* **12**, 2103-2107.

Breeuwer, P., Drocourt, J.L., Bunschoten, N., Zwietering, M.H., Rombouts, F.M. and Abee, T. (1995) Characterization of uptake and hydrolysis of fluorescein diacetate and carboxyfluorescein diacetate by intracellular esterases in *Saccharomyces cerevisiae*, which result in accumulation of fluorescent product. *Appl. Environ. Microbiol*. **61**, 1614-1619.

Chin-Joe, I., Nelisse, P.M., Straathof, A.J.J., Jongejan, J.A., Pronk, J.T. and Heijnen, J.J. (2000) Hydrolytic activity in baker's yeast limits the yield of asymmetric 3-oxo ester reduction. *Biotechnol. Bioeng*. **69**, 370-376.

Crotti, L. B., Drgon, T., Cabib, E. (2001) Yeast cell permeabilization by osmotic shock allows determination of enzymatic activities in situ. *Anal. Biochem*. **292**, 8-16.

Datta, J. and Samanta, T.B. (1992) Characterization of a novel microsomal glutathione *S*-transferase produced by *Aspergillus ochraceus* TS. *Mol. Cell. Biochem*. **118**, 31-38.

De Kimpe, N., de Cock, W. and Schamp, N. (1987) A convenient synthesis of 1-chloro-2-alkanones. *Synthesis* 188-190.

Grogan, G., Graf, J., Jones, A., Parsons, S., Turner, N.J. and Flitsch, S.L. (2001) An asymmetric enzyme-catalyzed *retro*-Claisen reaction for the desymmetrization of cyclic β-diketones. *Angew. Chem*. **113**, 1145-1148; *Angew. Chem. Int. Ed*. **40**, 1111-1114.

Guilbault, G.G. and Kramer, D.N. (1964) Fluorometric determination of lipase, acylase, α- and γ-chymotrypsin and inhibitors of these enzymes. *Anal. Chem*. **36**, 409-411.

Habig, W.H. and Jakoby, W.B. (1981) Assays for differentiation of glutathione *S*-transferases. *Methods Enzymol*. **77**, 398-405.

Iglesias, E. (1997) Determination of keto-enol equilibrium constants and the kinetic study of the nitrosation reaction of β-dicarbonyl compounds. *J. Chem. Soc. Perkin Trans. 2*, 431-439.

Jörg, G.; Hémery, T.; Bertau, M. (2005) Effects of cell-stress protectant glutathione on the whole-cell biotransformation of ethyl 2-chloro-acetoacetate with *Saccharomyces cerevisiae*. *Biocatal. Biotransform*. **23**, 9-17.

Jörg, G. and Bertau, M. (2004) Fungal aerobic reductive dechlorination of ethyl 2-chloro-acetoacetate by *Saccharomyces cerevisiae*: mechanism of a novel type of microbial dehalogenation. *ChemBioChem* **5**, 87-92.

Jörg, G., Leppchen, K., Daußmann, T. and Bertau, M. (2004) A novel convenient procedure for extractive work-up of whole-cell biotransformations using de-emulsifying hydrolases. *Biotechnol. Bioeng*. **87**, 525-536.

Naik, S., Gopinath, R., Goswami, M. and Patel B.K. (2004) Chemoselective thioacetalisation and transthioacetalisation of carbonyl compounds catalysed by tetrabutylammonium tribromide (TBATB). *Org. Biomol. Chem*. 2, 1670-1677.

Nakamura, K., Kawai, Y. and Ohno, A. (1990) A novel method to synthesize (*L*)-β-hydroxyl esters by the reduction with bakers' yeast. *Tetrahedron Lett*. **31**, 267-270.

Nishiyama, T., Matsui, S. and Yamada, F. (1986) Synthesis and spectral behavior of 5-methyl-3-phenyl-1,3-oxazolidin-2-ones using NMR. *J. Heterocycl. Chem*. **23**, 1427-1429.

Penninckx, M. (2000) A short review on the role of glutathione in the response of yeasts to nutritional, environmental, and oxidative stresses. *Enzyme Microb. Technol*. **26**, 737-742.

Schnürer, J. and Rosswall, T. (1982) Fluorescein diacetate hydrolysis as a measure of total microbial activity in soil and litter. *Appl. Environ. Microbiol*. **43**, 1256-1261.

Sartori, G., Ballini, R., Bigi, F., Bosica, G., Maggi, R. and Righi P. (2004) Protection (and deprotection) of functional groups in organic synthesis by heterogeneous catalysis. *Chem. Rev*. **104**, 199-250.

Schäfer, F.Q. and Büttner, G.R. (2001) Redox environment of the cell viewed through the redox state of the glutathione disulfide/glutathione couple. *Free Radical Biol. Med*. **30**, 1191-1212.

Schuster, S., Dandekar, T., Fell, D.A. (1999) Detection of elementary flux modes in biochemical networks: a promising tool for pathway analysis and metabolic engineering. *Trends Biotechnol*. **17**, 53-60.

Ushio, K., Ebara, K. and Yamashita, T. (1991) Selective inhibition of *R*-enzymes by simple organic acids in yeast-catalysed reduction of ethyl 3-oxobutanoate. *Enzyme Microb. Technol*. **13**, 834-839.

Wakil, S.J., Stoops, J.K. and Joshi, V.C. (1983) Fatty acid synthesis and its regulation. *Annu. Rev. Biochem*. **52**, 537-579.

Annex

Metabolic pathways of

ethyl acetoacetate (**AEE**)
ethyl 4-chloro-acetoacetate (**4CAEE**)
ethyl 4,4,4-trifluoro-acetoacetate (**FAEE**)

in *Saccharomyces cerevisiae*.

Metabolic Pathways of Ethyl acetoacetate in *Saccharomyces cerevisiae*

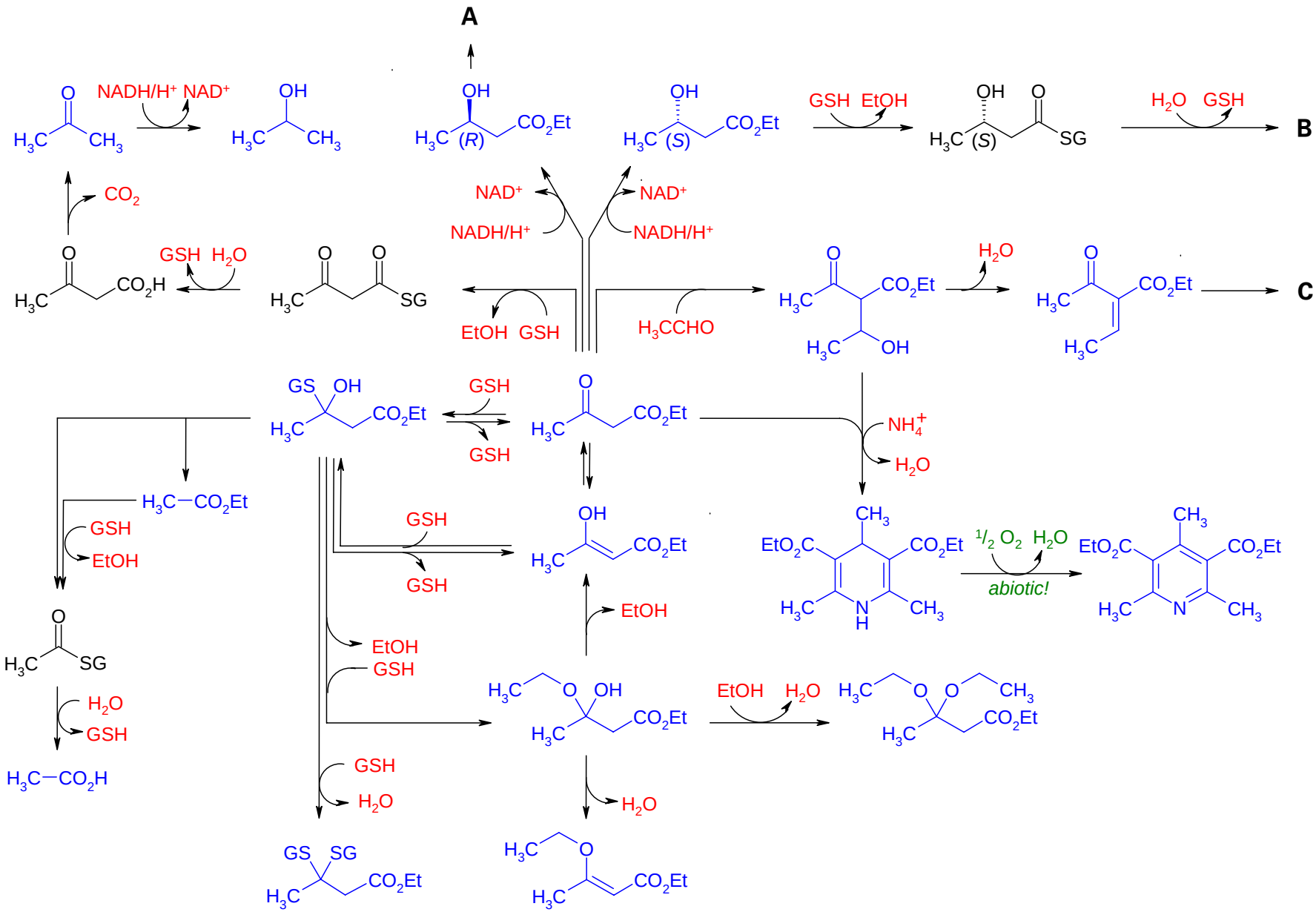

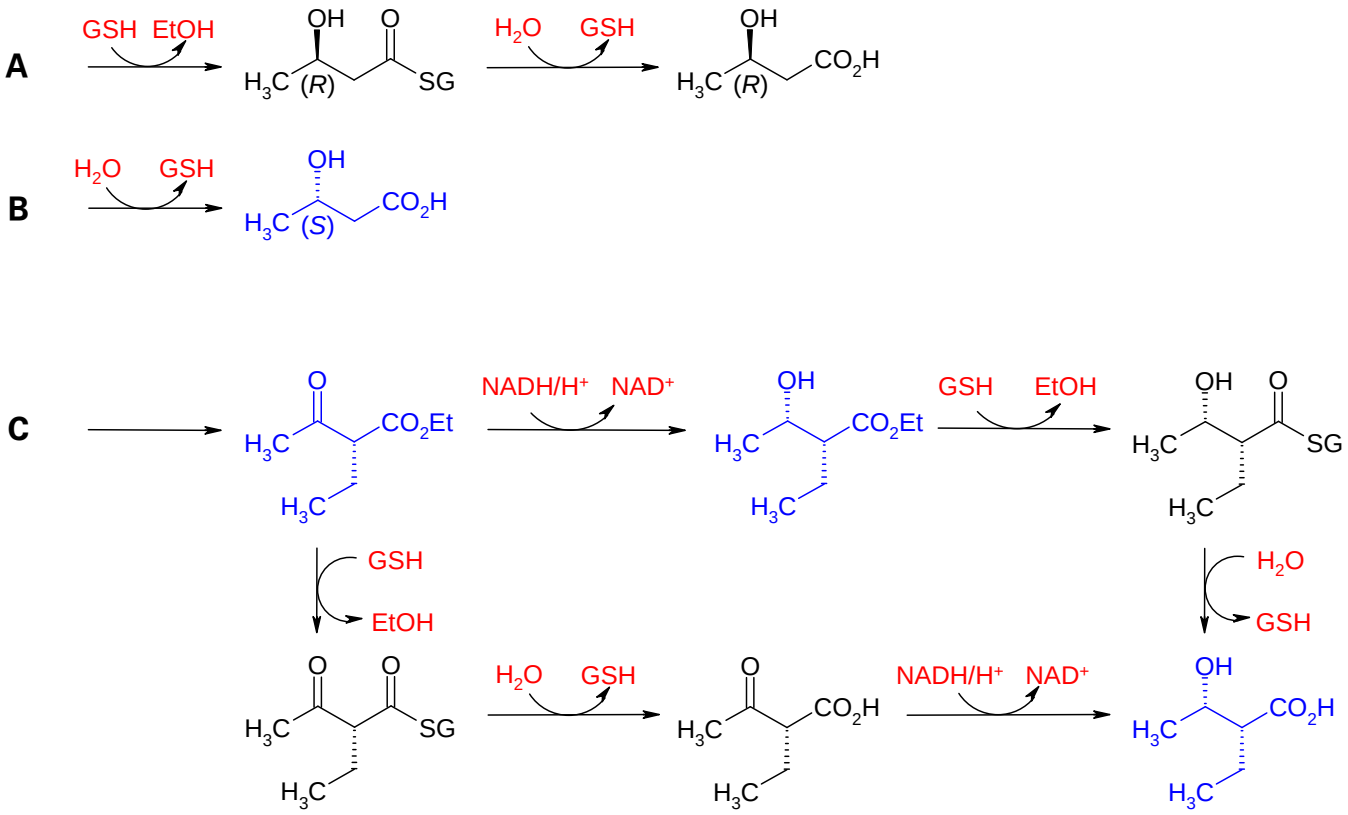
A
GSH EtOH
OH
O
H3C (R)
SG
H2O GSH
OH
H3C (R)
CO2H
B
H2O GSH
OH
H3C (S)
CO2H
C
O
CO2Et
H3C
H3C
NADH/H+ NAD+
OH
CO2Et
H3C
H3C
GSH EtOH
OH
O
H3C
SG
H3C
GSH
EtOH
H2O
GSH
O
O
H3C
SG
H3C
H2O GSH
O
CO2H
H3C
H3C
NADH/H+ NAD+
OH
CO2H
H3C
H3C

Metabolic Pathways of Ethyl 4-Chloroacetoacetate in *Saccharomyces cerevisiae*

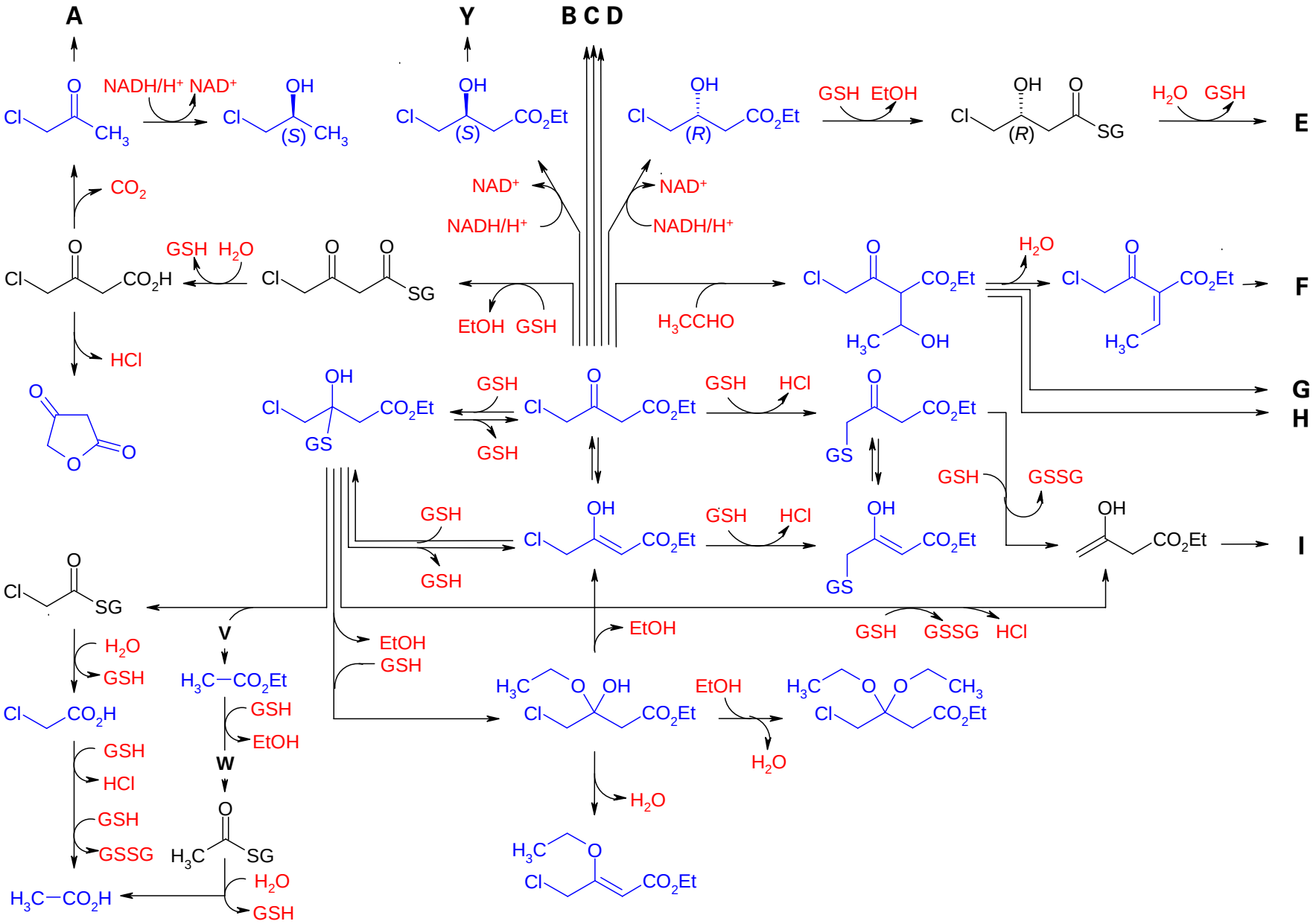

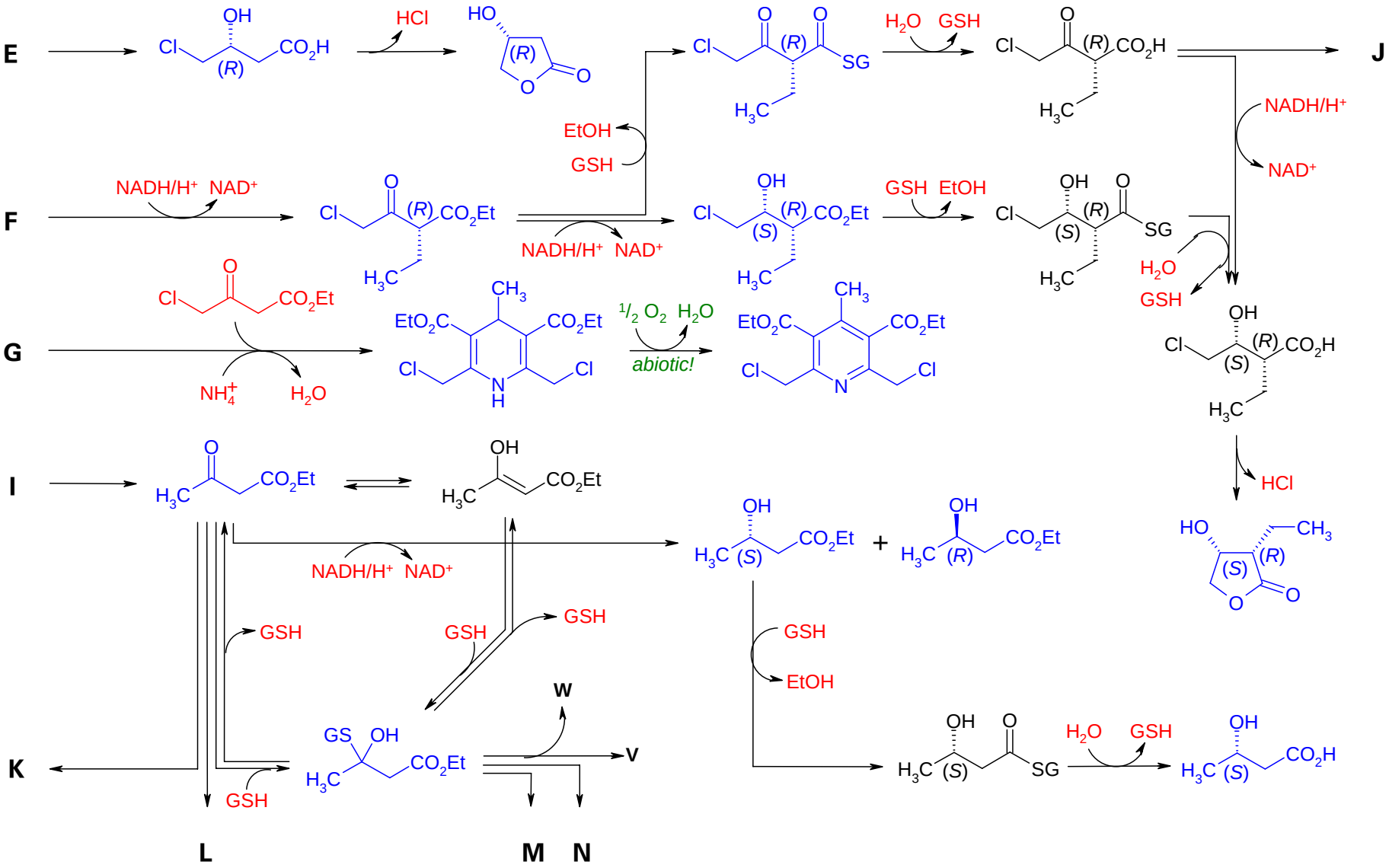
E
F
G
I
K
L
M
N
J
HCl
EtOH
GSH
NADH/H+
NAD+
H2O
GSH
EtOH
NADH/H+
NAD+
NH4+
H2O
1/2 O2
H2O
abiotic!
NADH/H+
NAD+
GSH
GSH
GSH
GSH
EtOH
HCl
H2O
GSH
w
v

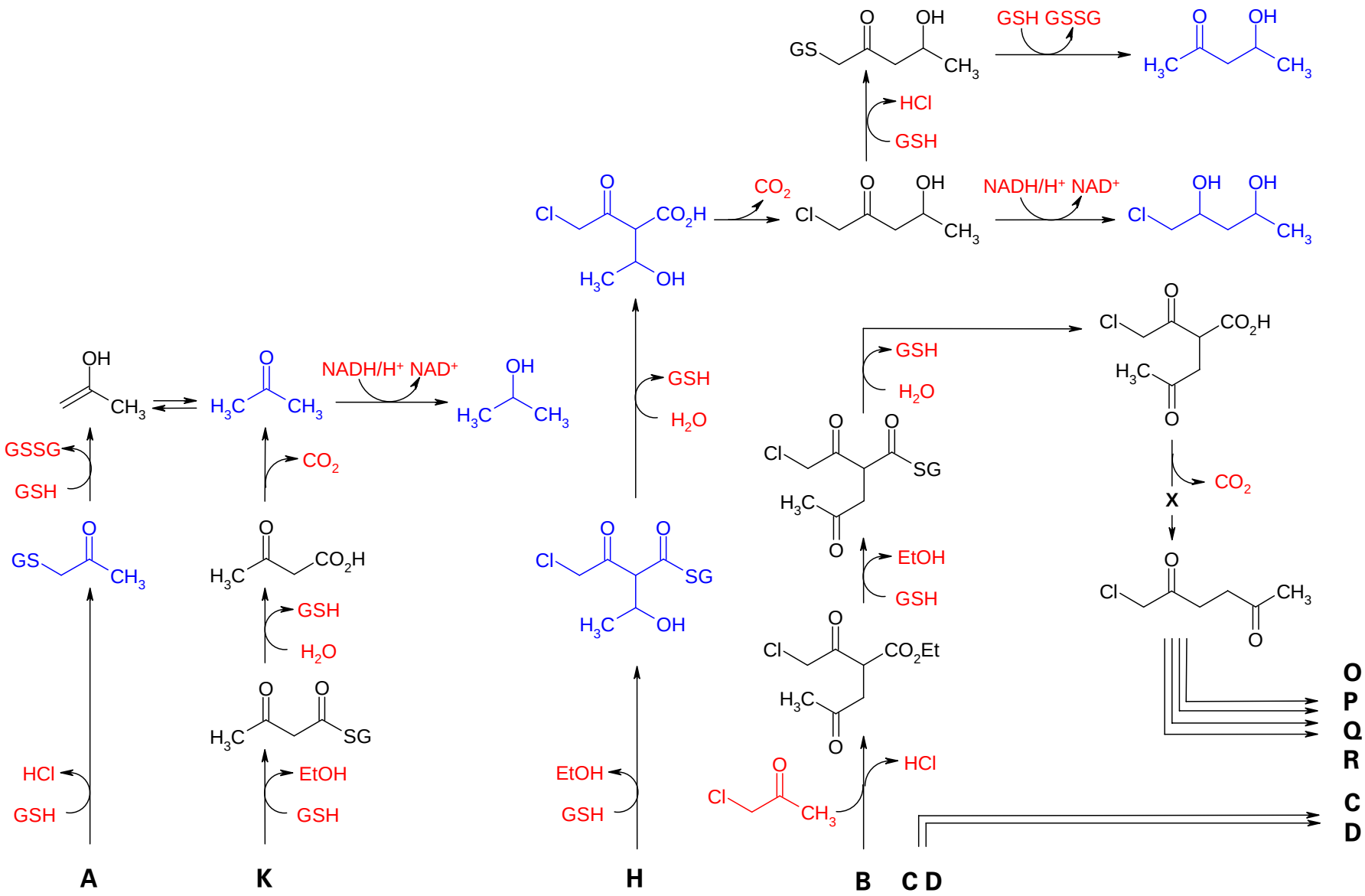
GSH GSSG
HCl
GSH
CO2
NADH/H+ NAD+
GSSG
GSH
CO2
GSH
H2O
EtOH
GSH
HCl
GSH
GSH
H2O
EtOH
GSH
HCl
X
CO2
O
P
Q
R
C
D
A
K
H
B
C D

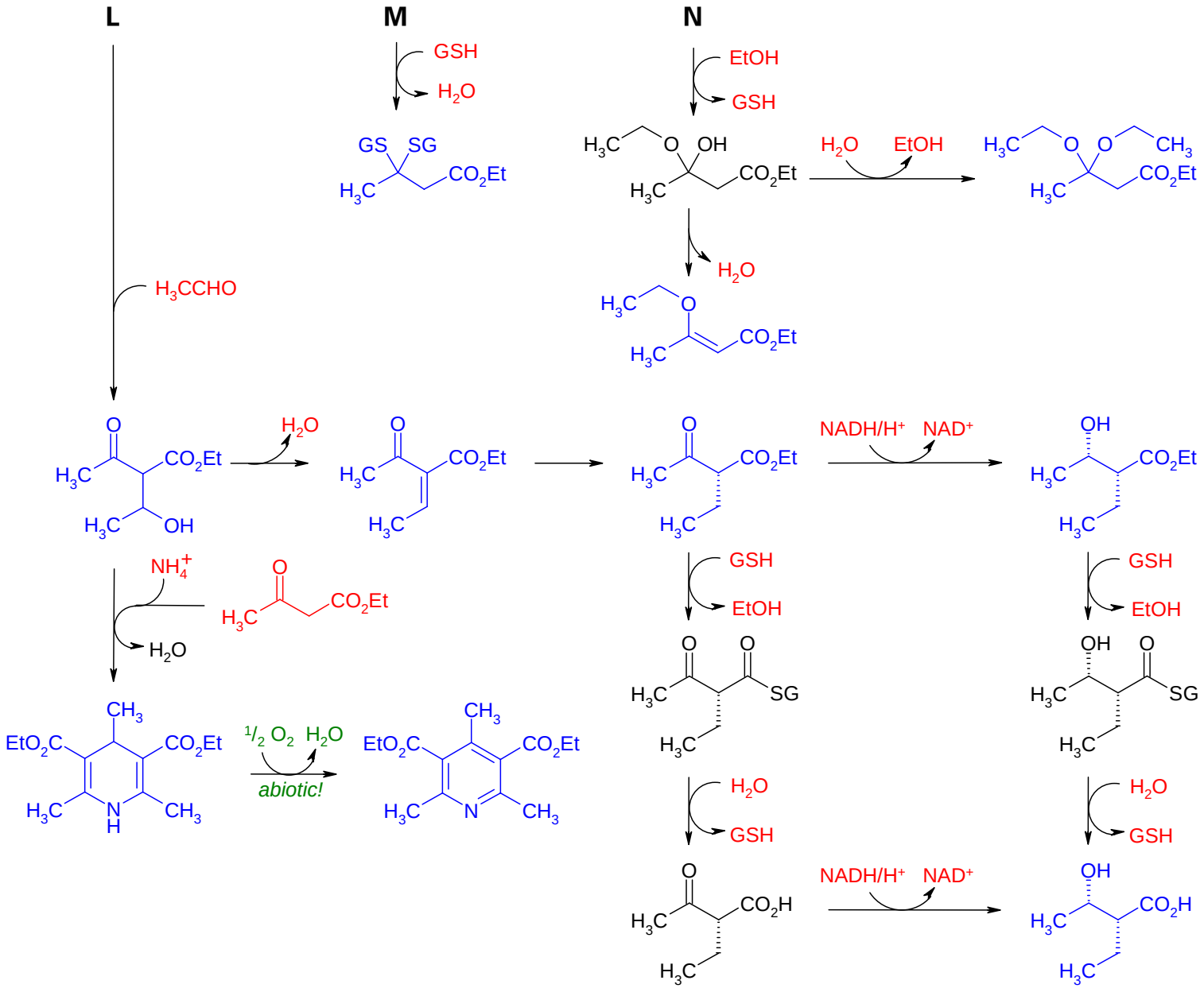
L
M
N
GSH
H2O
GS SG
H3C
CO2Et
EtOH
GSH
H3C O OH
CO2Et
H3C
H2O EtOH
H3C O O CH3
CO2Et
H3C
H2O
H3C O
CO2Et
H3C
H3CCHO
O
H3C
CO2Et
H3C OH
H2O
O
H3C
CO2Et
H3C
O
H3C
CO2Et
H3C
NADH/H+ NAD+
OH
H3C
CO2Et
H3C
NH4+
H2O
O
H3C
CO2Et
GSH
EtOH
O O
H3C
SG
H3C
GSH
EtOH
OH O
H3C
SG
H3C
CH3
EtO2C
CO2Et
H3C N CH3
H
1/2 O2 H2O
abiotic!
CH3
EtO2C
CO2Et
H3C N CH3
H2O
GSH
O
H3C
CO2H
H3C
NADH/H+ NAD+
H2O
GSH
OH
H3C
CO2H
H3C

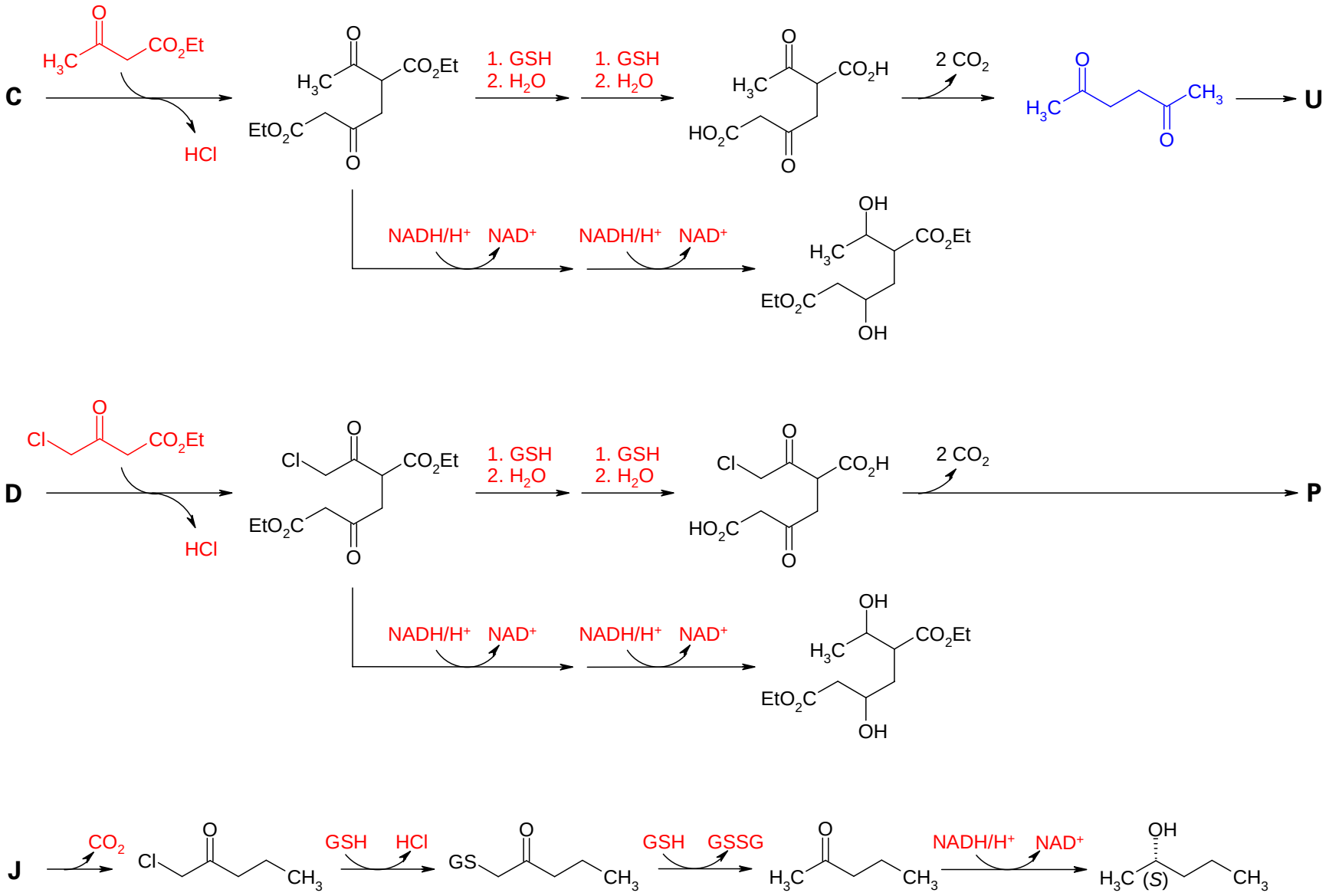
C
HCl
1. GSH
2. H2O
1. GSH
2. H2O
2 CO2
U
NADH/H+
NAD+
NADH/H+
NAD+
D
HCl
1. GSH
2. H2O
1. GSH
2. H2O
2 CO2
P
NADH/H+
NAD+
NADH/H+
NAD+
J
CO2
GSH
HCl
GSH
GSSG
NADH/H+
NAD+

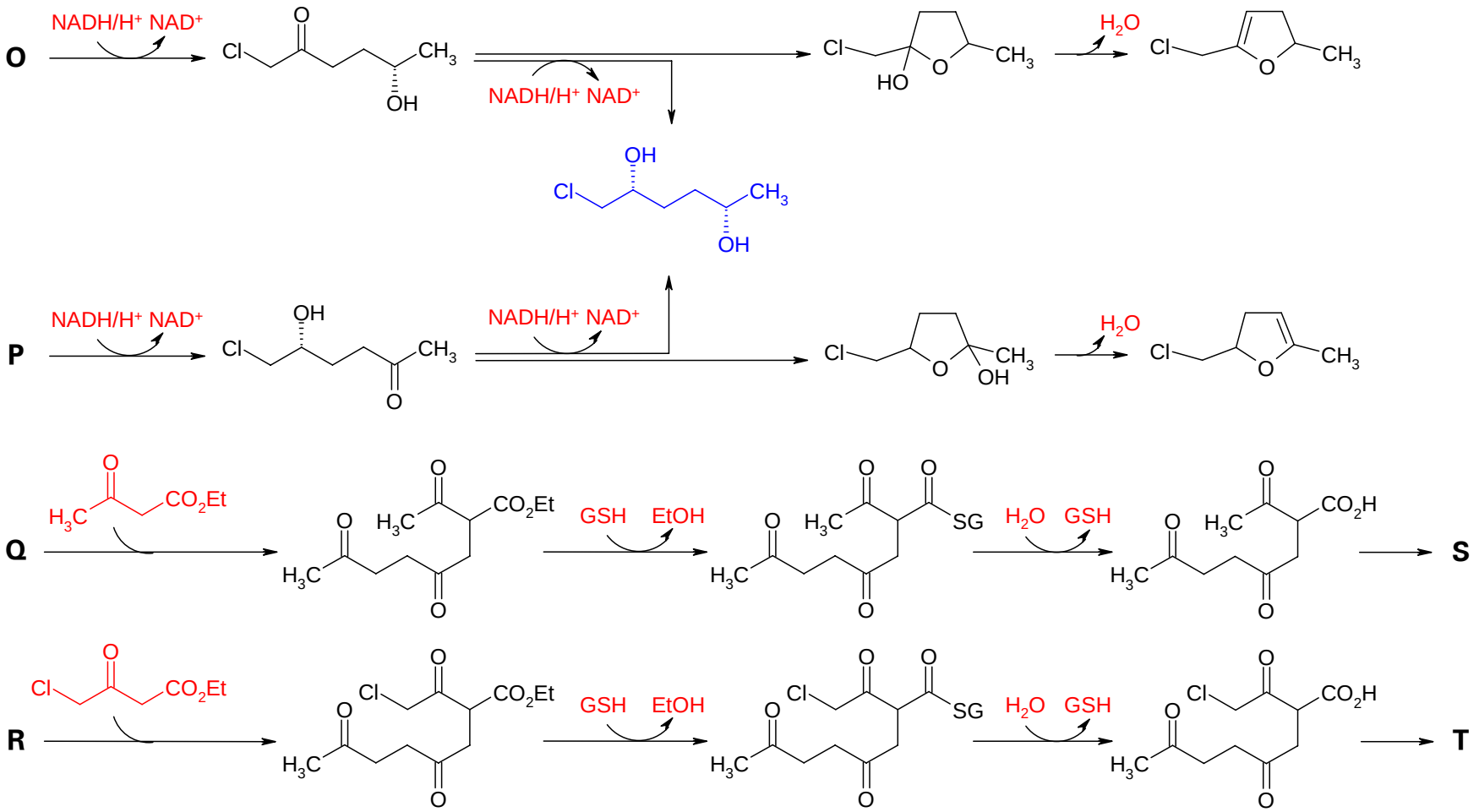
O
NADH/H+ NAD+
Cl
O
CH3
OH
NADH/H+ NAD+
Cl
HO
O
CH3
H2O
Cl
O
CH3
OH
Cl
CH3
OH
P
NADH/H+ NAD+
OH
Cl
CH3
O
NADH/H+ NAD+
Cl
O
CH3
OH
H2O
Cl
O
CH3
Q
O
H3C
CO2Et
O
H3C
CO2Et
O
GSH
EtOH
O
H3C
SG
O
H2O
GSH
O
H3C
CO2H
O
S
R
Cl
O
CO2Et
Cl
O
CO2Et
GSH
EtOH
Cl
O
SG
H2O
GSH
Cl
O
CO2H
T

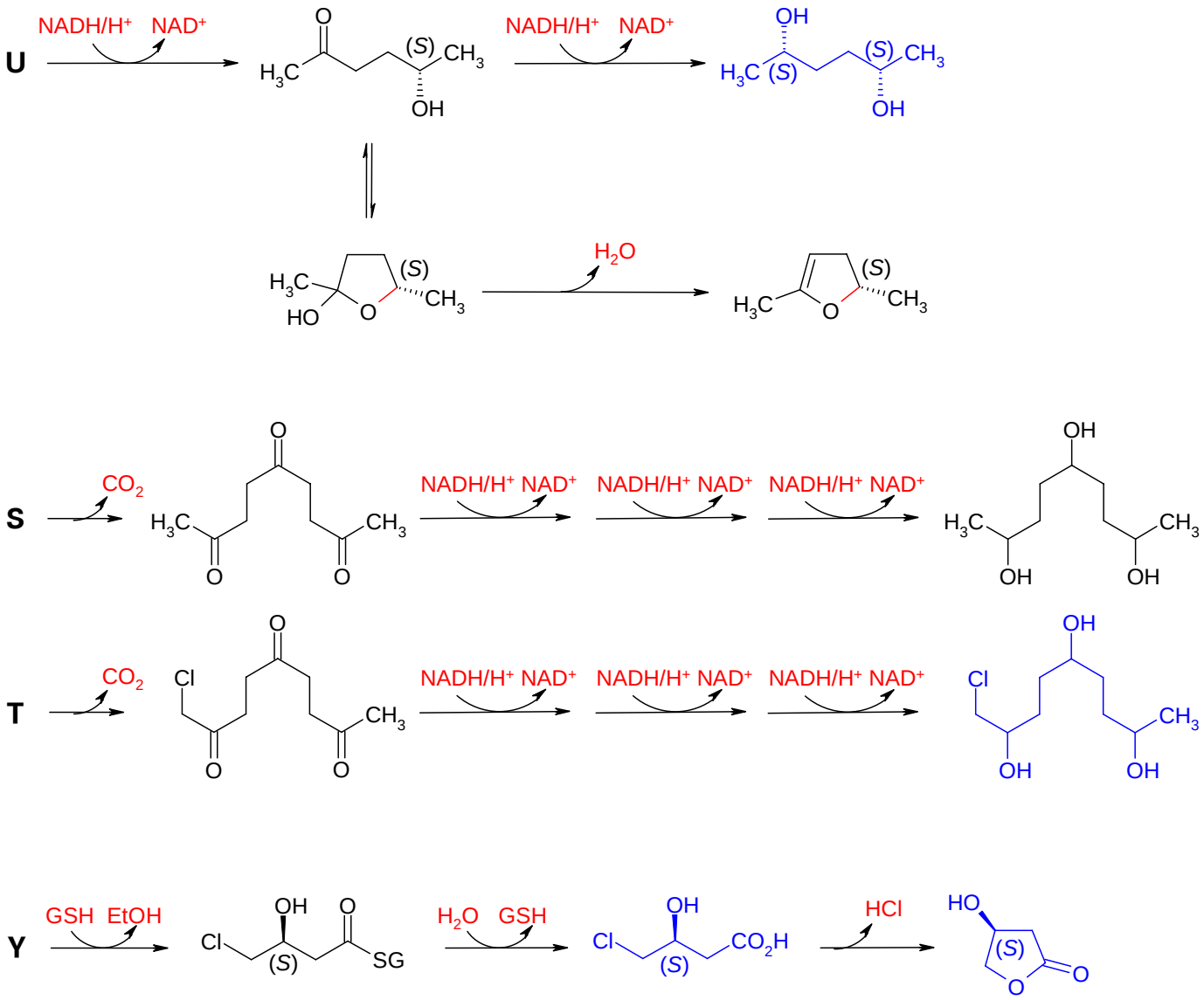
U
NADH/H+ NAD+
NADH/H+ NAD+
H2O
S
CO2
NADH/H+ NAD+
NADH/H+ NAD+
NADH/H+ NAD+
T
CO2
NADH/H+ NAD+
NADH/H+ NAD+
NADH/H+ NAD+
Y
GSH EtOH
H2O GSH
HCl

Metabolic Pathways of Ethyl 4,4,4-trifluoroacetoacetate in *Saccharomyces cerevisiae*

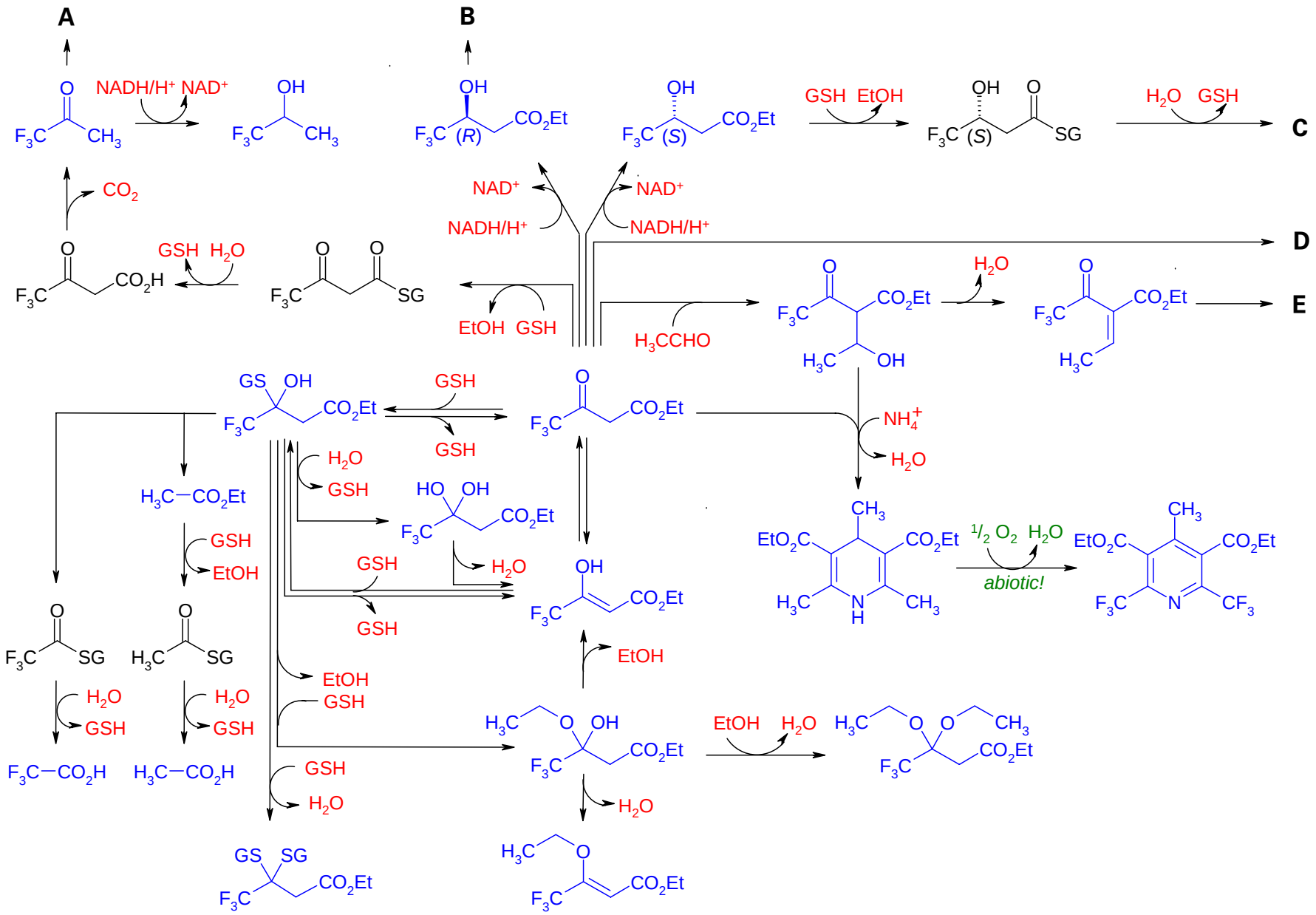

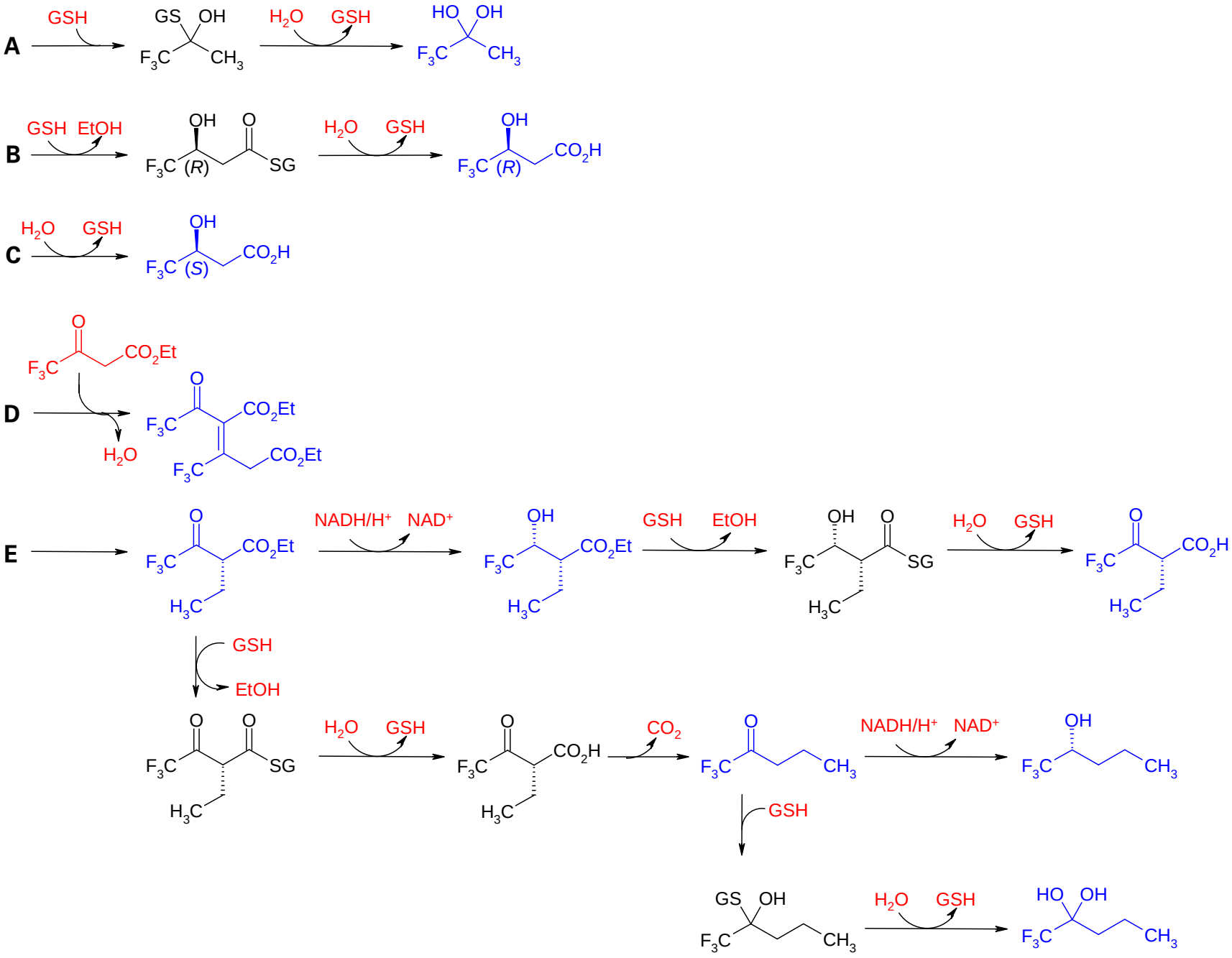
A
GSH
GS
OH
F3C
CH3
H2O
GSH
HO
OH
F3C
CH3
B
GSH
EtOH
OH
O
F3C
(R)
SG
H2O
GSH
OH
F3C
(R)
CO2H
C
H2O
GSH
OH
F3C
(S)
CO2H
D
O
F3C
CO2Et
H2O
O
CO2Et
F3C
F3C
CO2Et
E
O
F3C
CO2Et
H3C
NADH/H+
NAD+
OH
F3C
CO2Et
H3C
GSH
EtOH
OH
O
F3C
SG
H3C
H2O
GSH
O
F3C
CO2H
H3C
GSH
EtOH
O
O
F3C
SG
H3C
H2O
GSH
O
F3C
CO2H
H3C
CO2
O
F3C
CH3
NADH/H+
NAD+
OH
F3C
CH3
GSH
GS
OH
F3C
CH3
H2O
GSH
HO
OH
F3C
CH3